Ex-Core Thermo-Fluidic Modeling and Simulations for Transformational Challenge Reactor

P. Vegendla[1a], A. Bergeron[a], M. Subhasish[a], A. Talamo[a], F. Heidet[a]
B. J. Ade[b], B.R. Betzler[b]

[a)] *Argonne National Laboratory, 9700 South Cass Avenue, Argonne, IL 60439, USA*
[b)] *Oak Ridge National Laboratory, P.O. Box 2008, Oak Ridge, TN 37831-6170, USA*
[1] *svegendla@anl.gov*

INTRODUCTION

The safety of gas-cooled reactors must be ensured by active or passive cooling systems, which fulfill the task of keeping thermal loads on components and structures (i.e., vessel, confinement) within acceptable design limits under both normal and accident conditions. Thermo-Fluidics computer codes help designing, enhancing the performance and ensuring a high safety level for these cooling systems [1-2].

Using Computational Fluid Dynamics (CFD), a model of the Transformational Challenge Reactor (TCR) [3] ex-vessel and confinement was created in order to provide detailed information on the temperature distribution of ex-core components such as vessel, shroud, reflectors and bio-shield. The TCR program is using a rapid additive manufacturing approach to design, build, and operate a microreactor. The heat source values for these components were obtained from a detailed neutronic model of the TCR using the Monte Carlo code MCNP [4]. Based on these neutronics simulations, it was estimated that about 2.6 % of the total nuclear power is deposited ex-core (beyond the pressure vessel). If the in-core power is 3 MW, that represents about 80 kW deposited ex-core.

Several simulations were performed for various configurations using active air-cooling (forced) and natural circulation airflow. The STAR-CCM+® CFD commercial software [5] was used to model thermo-fluidic phenomena such as convective, conductive and radiative heat transfer.

The next section describes the numerical model of the TCR ex-core/confinement and the section after that focuses on results and analysis of the two aforementioned cases: active air-cooling and natural circulation airflow.

NUMERICAL MODELING

The ex-core geometry consists of several components: reactor pressure vessel (RPV), shroud, reflectors, concrete/bio-shield, heat exchanger and confinement walls. The CFD model was built with and simulations were performed using the STAR-CCM+® code.

The axisymmetric CFD model created for the TCR confinement/ex-core simulations is shown in Figure 1. The heat exchanger and support structures for RPV, reflectors and heat exchanger are modeled as porous bodies and assumed to consist of 50% air and 50% steel volume fraction due to limited available data. In porous bodies the inertial and viscous flow resistance are set to zero.

In natural circulation airflow configuration, the perfect closed confinement was considered in which the air recirculates due to buoyancy (density variations) effect. In active air-cooling configuration, the inlet coolant duct was placed beneath the RPV where the blower drives the specified air mass flow rates into the confinement. The hot air is removed via two vent/outlet ducts, which are placed over the confinement roof. In both configurations, the heat is removed via convection, conduction and thermal radiation.

Modeled Details and Boundary Conditions

The STAR-CCM+® code uses the finite volume (FV) method to solve the Navier-Stokes fluid flow equations numerically. In STAR-CCM+, the velocity and k-omega turbulence equations were solved using steady state, real gas, non-isothermal, segregated flow solver [5]. Also, the buoyancy effects are included by adding gravity term. The grey thermal surface-to-surface radiative heat transfer model was selected. The emissivity of the bio-shield and rest of the components were set at 0.94 and 0.8, respectively, which is considered a reasonable hypothesis. Temperature-dependent thermal physical properties such as thermal conductivity, specific heat and density were implemented for both fluid and solid components.

In Table I, the operating conditions are presented. In both active and natural circulation airflow, the environment boundary condition (ambient air temperature) were specified at confinement walls except the ground floor. The convective heat transfer coefficient for the confinement wall boundaries were set to be 20 W/m^2-K, which was considered a reasonable value. For the RPV, a constant temperature boundary condition was specified for the inside wall (573 K). In addition, the conductive heat transfer boundary condition was specified for all support structures, which are in direct contact with the ground floor.

In forced air circulation, a pressure boundary condition was specified at the outlet, flow velocity and temperature were specified at inlet, and a no-slip boundary condition was imposed at walls.

The volume mesh was generated to simulate the confinement configurations as shown in Figure 1. The minimum volume edge size was 2 mm over the vessel, shroud and reflector surfaces and the maximum cell edge size was allowed up to 80 mm near the confinement wall surfaces. In addition, three volumetric control blocks were introduced to control the mesh size around the bio-shield, reflector and shroud and vessel structures. This produces a finer mesh with a relatively uniform cell size, helping to prevent numerical instabilities and the maximum cell edge size was kept at 4.8 mm, 9.6 mm, 20 mm, respectively. A total of four prism layers were selected over the fluid-wall surfaces with a total thickness of 2 mm. The total number of generated mesh cells is close to 10 million (figure 2). In addition, the mesh was refined (~13 million) and simulations performed to ensure the present results are grid independent (not shown due to negligible differences).

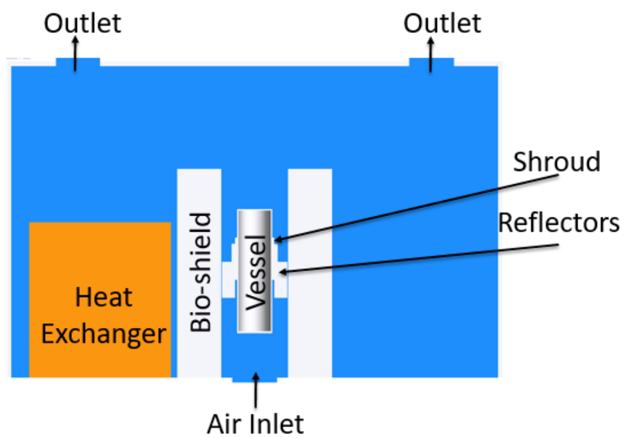

Fig. 1. Ex-core geometry configuration for active air-cooling.

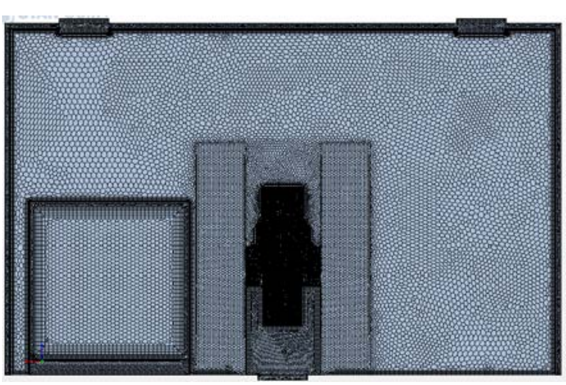

Fig. 2. Ex-core mesh configuration for active air-cooling.

TABLE I. Operating conditions

Component	Value
RPV inside wall temperature [K]	573
Ex-core total heat source [kW]	84
Thermal specification for all walls, except floor	Environment
Ambient temperature [K]	300
Convective heat transfer coefficient [W/m^2-K]	20
Active air-cooling mass vol. flow rate [m^3/s]	6.53

RESULTS

In this section, active air-cooling and natural air circulation results are presented. The results are provided for specified power distribution profiles for the RPV, shroud, reflectors, bio-shield and its support structures.

Figure 3 shows the velocity distribution in active air-cooling and natural air circulation flows. In natural circulation airflow, the hot air raises towards the roof where heat is exchanged with the environment and the cold air recirculates towards the bottom of the heat structures. The heat removal rate (~100 times higher heat transfer coefficient near the vessel, shroud and reflectors in active air-cooling) is not efficient when compared to active air-cooling due to the limited air re-circulation. The limited air-circulation was mainly due to the narrow flow channels between the solid components and the bio-shield. The bio-shield is radially closed from the ground.

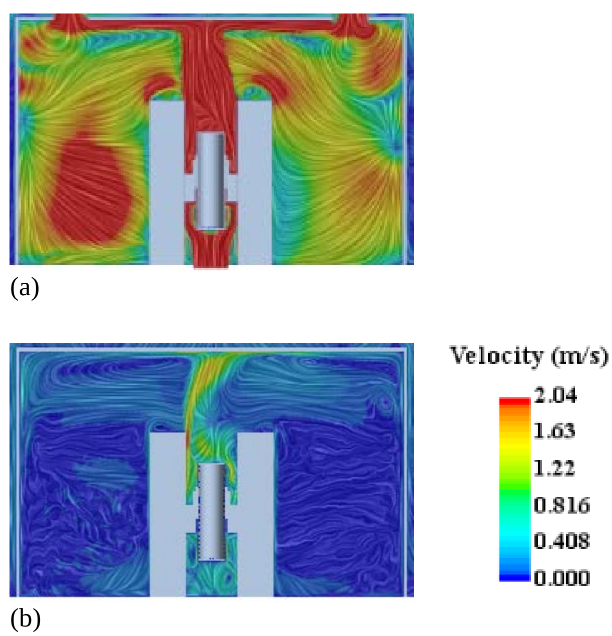

Fig. 3. Ex-core fluid velocity contours over XZ-plane; (a) Active air-cooling and (b) Natural circulation airflow.

In Figures 4-5, the temperature distributions are shown in vertical planes (YZ and XZ-plane) for both active air-cooling and natural circulation airflow. The significant temperature drop was observed in active air-cooling configuration (Table II). In solid components, the maximum predicted temperatures are within the designed specification limit. However, further optimization analyses are needed to minimize the air mass flow rates and develop efficient heat removal designs for heat deposited in components such as shroud, reflectors and bio-shield, even under normal operating conditions. To be noted, the bio-shield and the rest of the components (shroud, RPV and reflectors) safety design temperature limits are 430K and >1000 K, respectively.

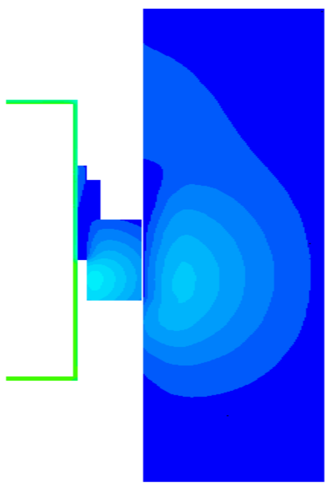

(a)

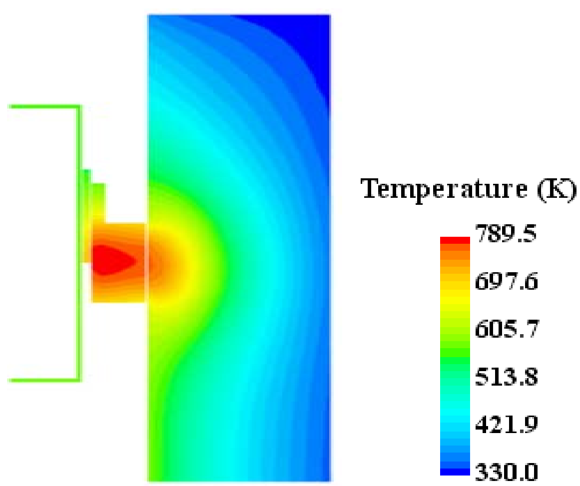

(b)

Fig. 4. Ex-core solid temperature distribution over YZ-plane; (a) Active air-cooling and (b) Natural circulation airflow.

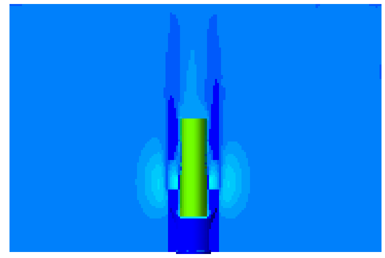

(a)

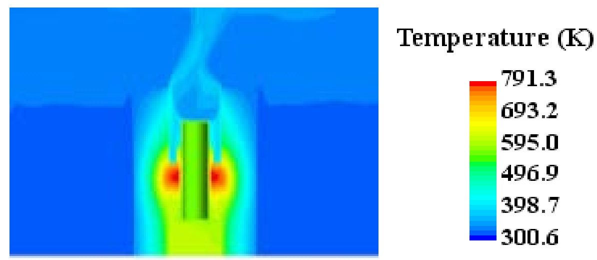

(b)

Fig. 5. Ex-core fluid and solid temperature distribution over XZ-plane; (a) Active air-cooling and (b) Natural circulation airflow.

TABLE II. Maximum predicted solid temperatures

Component	Active air-cooling temperature [K]	Natural circulation temperature [K]
RPV	573	604
Shroud	363	716
Reflector	437	771
Bio-shield	408	796

In active air-cooling, the heat transferred from RPV inside wall surface to outer wall surface due to forced air-cooling (low temperatures). In contrast, the heat transferred from RPV outer wall surface to inner wall surface due to higher temperatures than the RPV inside wall surface boundary condition.

CONCLUSIONS

3D CFD simulations were performed to analyze the TCR ex-core temperature distribution for both active air-cooling and natural circulation airflow. In active air-cooling, the observed maximum temperatures were within the designed safety limits for bio-shield, reflectors, shroud and RPV. In contrast, the observed temperatures were far from the designed safety limits for the case using natural circulation airflow. Future work involves the thermal optimization of new configurations for ex-core components due to continued evolution of TCR designs and its new requirements.

ACKNOWLEDGMENTS

The Transformational Challenge Reactor program is supported by the U.S. Department of Energy Office of Nuclear Energy (DOE-NE). The submitted manuscript has been created by UChicago Argonne, LLC, Operator of Argonne National Laboratory (“Argonne”). Argonne National Laboratory’s work was supported by the U.S. Department of Energy, Office of Nuclear Energy under contract DE-AC02-06CH11357.

REFERENCES

[1] E. Studer et al. “CAST3M/ARCTURUS: A coupled heat transfer CFD code for thermal–hydraulic analyzes of gas cooled reactors”, *Nuc. Eng. & Des.*, 237, pp. 1814–1828 (2007).

[2] C.H. Oh et al. “Development Of Safety Analysis Codes And Experimental Validation For A Very High Temperature Gas-Cooled Reactor”, Idaho National Laboratory, INL/EXT-06-01362, (2006).

[3] K.A. TERRANI, “Transformational Challenge Reactor Demonstration Program,” (2019). Retrieved from http://tcr.ornl.gov.

[4] C.J. WERNER (editor) et al., “MCNP6 User’s Manual, Code Version 6.2”, Los Alamos National Laboratory, LA-UR-17-29981, (2017).

[5] Simcenter STAR-CCM-v19.02, USER GUIDE, https://www.plm.automation.siemens.com/global/en/products/simcenter/STAR-CCM.html.